

Sampling of Atmospheric Aerosols by Electrostatic Precipitation for Direct Analyses

Gerd Hermann^{1*}, Georg Lasnitschka¹, Rudolf Matz¹, Alexander Trenin¹ and Walter Moritz²

¹ I. Physikalisches Institut, Justus-Liebig-Universität Gießen, Heinrich-Buff-Ring 16, D-35392 Giessen, Germany

² Fa. Grün-AMS GmbH, D-35630 Ehringshausen, Germany

*Corresponding author (gerd.hermann@exp1.physik.uni-giessen.de)

Abstract. A novel system for aerosol sampling by electrostatic precipitation using graphite platforms as sample collector is presented. Employing standard platforms for commercial analytical instruments, the conception allows fast solid sampling direct element analysis with ETAAS, ETV-ICP-MS/OES, and ETACFS without any wet digestive pre-treatment. Other advantages are: highly efficient electrostatic particle collection (>99% for $d = 10 \text{ nm}-10 \mu\text{m}$), reusable sample collectors, omission of filters and chemical reagents. On this basis, an electrostatic precipitator is constructed aiming at a small, relatively uncomplicated instrument. Ten precipitators are arranged in a multi-sampling apparatus for outdoor operation, which simultaneously collect ten samples on same or different collectors for instrumental element analyses, or for microscopic investigations of the collected particles. The precipitator is tested with different model aerosols as well as with atmospheric sampling. Element analysis is carried out with the above mentioned solid sampling methods in external as well as in the authors laboratories.

Keywords: Aerosol analysis; electrostatic precipitation; corona discharge; element analysis; solid sampling; boat technique; graphite platform; scanning electron microscopy; SEM

2.2 Smaller particle sizes

Since there are several advantageous approaches for collecting particles of large sizes, as with impactors or cyclones, and since ETV is suited for highly efficient precipitation of large as well as of small particles, main interest has been focused on electrostatic collection of particles with aerodynamic diameters $<1\text{ }\mu\text{m}$. Test aerosols with particulates down to 5 nm have been generated with a laboratory constructed arrangement by vaporizing sample material in an electrically heated graphite tube with subsequent particle condensation on the axis of a vertical convection tube. The arrangement is shown in Fig. 5. Obtained particle sizes and structures depend on the composition and concentration of the vaporized material. As primary substances liquid dosed solutions as well as solids have been used.

Aerosols with particle sizes in the range of such small diameters were also obtained by laser ablation from solids, such as metals, ceramics, and carbon or plastic materials. Employing a continuously pumped Nd: YAG laser, pulse frequencies of some shots per second up to 4 kHz could be applied without loss of pulse intensity. Thus, by scanning the surface of the evaporated material with an x-y-drive, a continuous aerosol flow of over hours constant composition can be provided as model aerosol.



Fig. 5: Laboratory constructed electrothermal vaporizer with upstream for efficient axial focused condensation (AFC), generating particulates with $d = 5\text{ nm}-1\text{ }\mu\text{m}$

For SEM, platforms or disks of GC, HOPC, and of silicon cut from Si wafers have been employed as substrates. For transmission electron microscopy copper nets covered with a thin organic film have been used. Fig. 6 presents SEM micrographs of electrostatically precipitated aerosols obtained with different compositions and masses of the vaporized primary sample. First row (Figs. 6.1a–6.1c) shows the precipitation obtained with vaporizing a sample dosed to the ETV boat as aqueous multielement solution containing

Ag, Pb, Cu, Fe, Al, and Ni (concentrations see in figure caption) onto a GC substrate. Fig. 6.1a shows an overview over the whole precipitation area, which is limited to a nearly circular area of about 1.5 mm in diameter. The circular symmetry is slightly perturbed in the direction, where the wire tip of the discharge is assumed to be at the inner wall of the jet capillary. Micrographs with higher magnification (Figs. 6.1b–c) show the particle spectrum from 20 nm up to more than 1 μm , in this case, with mostly amorphous, and coagulated flake-like structures. The sample of Figs. 6.2a–c is collected on the same GC substrate with the same multielement solution but in this case with additional high content of Zn and Cd (1 μg and 320 ng, respectively) dosed as primary sample to the ETV boat. The particle sizes are larger and show more crystalline particle structures. Figs. 6.3a–6.3c show that adding of a higher amount of potassium to the same solution as in 6.1a–6.1c results in growing of a larger number of smaller particles. Our interpretation is that this is owing to the fact that potassium has low ionization energy and that a high fraction of K is released from the furnace as ions, which quicken the condensation process. The micrographs of the fourth row demonstrate the effect of the gas flow, which is reduced from 1500 to 150 ml/min. The dosed element masses are 1/5 of those in second row and with 1 μg K as in the third row. Owing to the reduced flow, larger and more crystalline particles are obtained.

Last row (Figs. 6.5a–5c) shows samples obtained by precipitation of aerosols generated from steel with laser ablation. The substrate of Fig. 5a is a commercially available pyro-graphite platform (for HGA 600, Bodenseewerk Perkin Elmer, GmbH). Aerosols obtained by laser ablation with low pulse energies ($\sim 100\text{ }\mu\text{J}$) are similar to those by ETV. With higher pulse energies additional larger sized spherical particles are generated by pressure spraying effects from the molten solid surface in the laser spark, which results in small droplets with diameters of some hundred nanometers up to some micrometers. Figs. 6.5b–c present high resolution Transmission Electron Micrograph (TEM) showing that the diameters range down to $<10\text{ nm}$ like those obtained with ETV generated aerosols. These micrographs show a high number of small particles typically 5–10 nm in diameter. In the right bottom corner of Fig. 6.5b a sector of a spherical particle is shown with about 0.3 μm in diameter; another spherical particle with 60 nm in diameter can be seen near the center below the upper margin of this picture. The large particles are precipitated by superimposed electric and inertial forces, and predominantly appear directly in the center area of the deposition zone. The smaller particles of some 5–50 nm shown on Fig. 6.5b and 6.5c are of about the same size as those obtained with ETV.

The investigations show that the particle sizes of model aerosols generated with ETV depend on many parameters as material composition, gas flow, temperature gradient, density of vaporized material and can be chosen by adequate choice of these parameters. By means of LA with a pulsed laser system quasi-continuous aerosol flows can be obtained. The micrographs show that aerosols with particle diameters

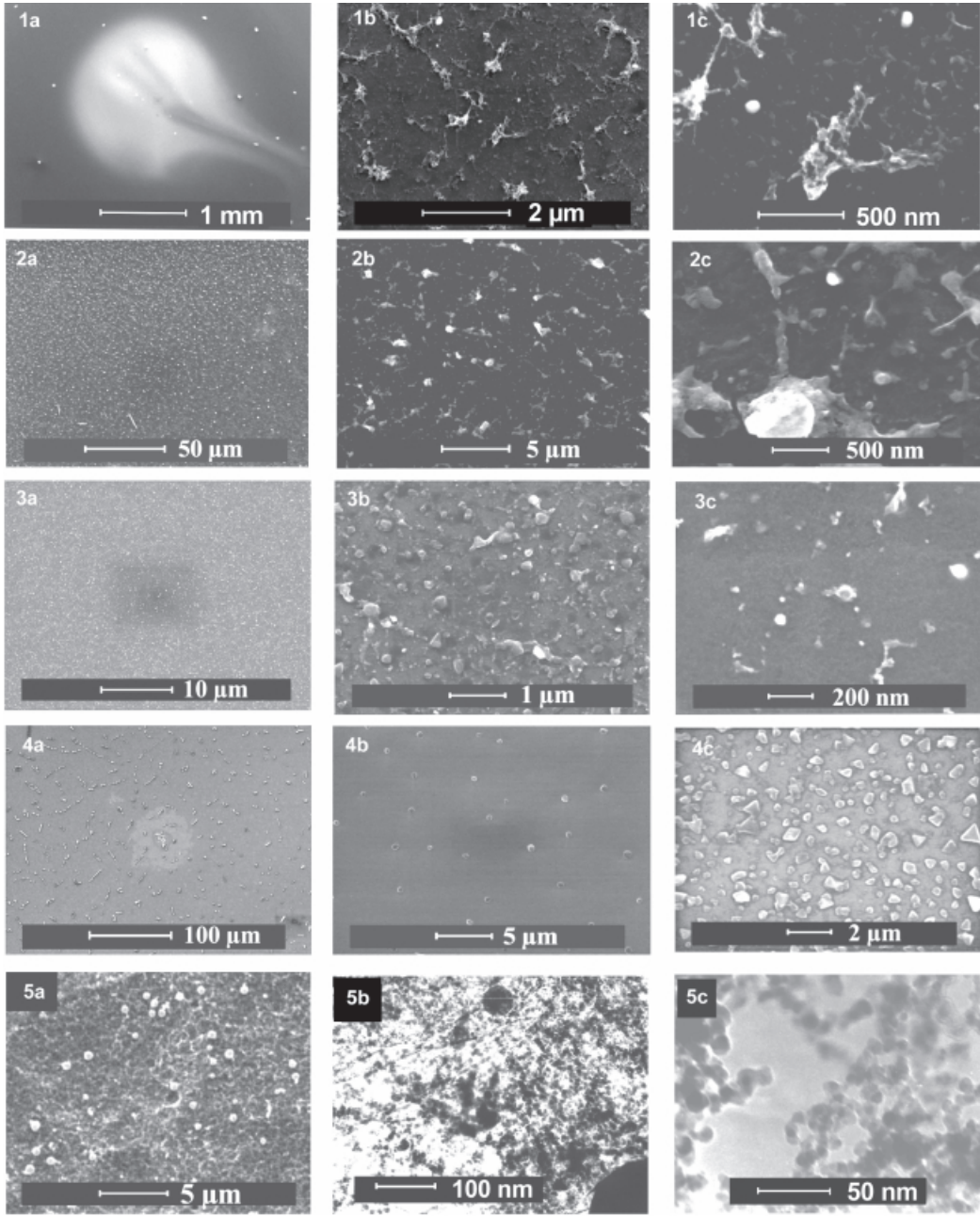


Fig. 6: Micrographs of EP obtained with model aerosols generated with ETV (upper 4 rows, Figs. 6.1a–6.4c, SEM: Philips XL 30) and with laser ablation (last row, Figs. 5a–5c, TEM: Philips CM30). First row 1a–c: vaporization of a sample containing 10 ng Ag, 32 ng Pb, 32 ng Cu, 64 ng Fe, 32 ng Al, 320 ng Ni, dosed to ETV boat as nitric acid solution, ETV flow 1.5 l/min, flow splitting: 1/10 of generated flow piped to the precipitator; 2a–2c: same as before, however, with additional content of 1 μg Zn and 320 ng Cd; 3a–3c: same as 1a–1c, but with additional content of 1 μg K; 4a–4c: containing 1/5 of masses of 2a–2c plus 1 μg K, ETV flow 150 ml/min; last row: Laser Ablation of steel, 5a: SEM, substrate pyro-graphite platform produced for using in AAS instruments, 5b–5c: TEM with steel, substrate: copper net covered by organic thin film

from less than 10 nm up to several micrometers can be generated and electrostatically precipitated on the deposition zones of the collectors. Analytical determinations with the electrostatically recollected ETV generated model aerosols are possible as well. The precipitated masses can be related to the primary masses dosed to the ETV boat. With such evaluation, these ratios are 40–80%. However, the main

losses of these complete ETV-EP cycles occur during the vaporization, condensation, and aerosol transport processes. Thus, such over-all efficiencies are by far too low estimates for the EP efficiency. The measurements with the cascaded two-stage precipitators with and without corona applied to the first stage give more reliable results.

3 Results and Discussion with Atmospheric Aerosols

Employing the ten-fold multi-sampler shown in Fig. 3, atmospheric aerosols could be collected on up to ten substrates simultaneously. Sample boats for element analyses with different state-of-the-art instruments can be employed simultaneously together with substrates for optical microscopy and for SEM. The ten stations can be loaded with the same or different substrates for the required instruments: For SEM, graphite platforms, Si plates, HOPC, or GC, for optical microscopy glass plates with conductive ITO layers.

Fig. 7 shows micrographs of the particles of a 'clean air' aerosol precipitated on October 11th 2000 at the observation station 'Kleiner Feldberg', Rhine-Main area, Germany. The air inlet was taken via a PM 5 elutriator. As substrate a single crystal silicon plate 5x15x1 mm in size was used. The sampling time was 6 h with a partial airflow of 150 ml/min

for each precipitator. Owing to the place in a low-mountain woodland area, relatively apart from traffic and industry, major organic composition of the particulates is to be expected. Fig. 7a shows the full precipitation zone that is about 1.5mm in diameter. The precipitation is clearly fractionated (see Figs. 7a and 7b) owing to the different electric mobility, decreasing from zone 'A'-'D', due to different sizes, structures, and charges of the particles similar as with a mobility analyzer [15]. There is a small center zone ('A' in Fig. 7a) of about 250 μm in diameter where all sizes of the particle spectrum from diameters below 200 nm up to 5 μm are found.

Next micrographs show zone 'A' (see Fig. 7.1c) and details of zone 'A' (see Figs. 7.2a–7.2c) with higher magnification. For the larger particles precipitated in the central zone, a major effect of inertial forces is superimposed to the electrostatic forces. The larger structures in Figs. 7.2a–b are re-

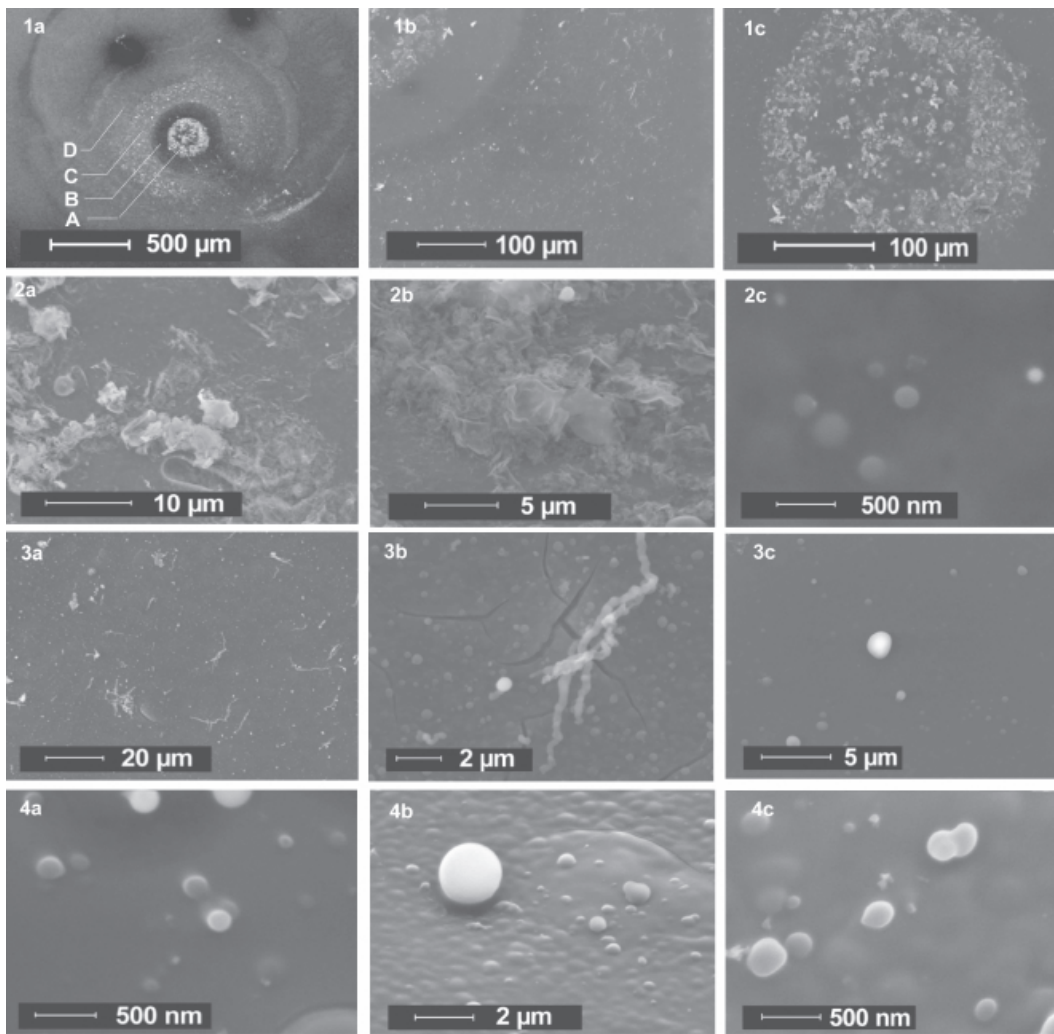


Fig. 7: SEM micrographs (Philips XL20) of the particles precipitated of a 'clean air' aerosol; substrate: silicon; sampling time: 6 h; air flow per precipitator: 150 ml/min; 1a)–4a) without, 4b–c) with gold coating. 1a) full overview showing circular areas; 1b) overview showing the radial course of particle structures; 1c): center zone ('A') with higher magnification; 2a)–2b): particles in zone 'A' with higher magnification; 2c): smaller particles in zone 'A' that also cover zones 'B'–'D'; 3a)–3b): 'fibrous' particles (Actinomycetes) of zone 'C' together with the smaller spherical particles spread over 'A'–'D'; 3c): non-fibrous particles in zones 'C'; 4a) smaller spherical particles in zone 'C' at higher magnification; 4b–c): SEM after gold coating on zone 'D', better showing the spherical or flat character, respectively

garded to be of organic origin, such as organic membranes. On places between the larger particles, much smaller, more or less spherical particles can be seen on the micrographs. Fig. 7.2c shows such particles in zone 'A'. Particles of this kind are also found on the zones 'B', 'C', and 'D'. Zone 'B' shows a much lower mass density and contrast than the neighbouring areas. It is covered with the smaller particles. A lot of fibrous material is on the circular precipitation area 'C'. Figs. 7.3.a–b show such particles in zone 'C'. These fibrous particles are recognized as Actinomycetes [16]. Part of the smaller circularly appearing particles spread over the zones 'A'–'D' (see Figs. 7.2c, 7.3c–7.4a) seems to be very flat with low contrast in SEM, some others appear spherical with higher contrast. The flat circular particles are interpreted as dried moist particles, such as droplets of nebular clouds, containing more or less dissolved material. In order to show the relief structure better and to present the contrast independently from the particle material, Figs. 7.4.b–c) show SEMs with gold-layered surface. It is taken in the area between 'C' and 'D' and better shows the contours of the different particles. Part of these particles is also expected to be organic, such as spores and hyphae. The fractionation of the deposition owing to the different electrical mobility shows that very different types of particles and shapes may be found in one mobility class. Outside the precipitation area of about 1.5 mm in diameter the surface is clean, no particles are found.

Analytical determinations employing graphite platform boats as sample collectors were carried out with solid sampling multi element CS-CFS, SSAAS, ETV-ICP-MS. Multielement CS-CFS has been carried out in a wavelength range 285–330 nm. The sample has been introduced into the furnace via ETV and re-

precipitated inside the CFS furnace with EP (ETV-CS-CFS). In this wavelength range, lines of the elements Mg, Si, Mn, Fe, Al, Cu, and Ca could be detected with all samples collected during the campaign on 'Kleiner Feldberg'.

With the chosen sampling times, the concentrations of Si, Ca, and Mg were so high that the CFS intensities were saturated on these lines. For these elements and with chosen sampling volumes, lowest mass limits could be given, only. The other elements were in the analytical range and could be determined. Results are presented in Table 1 together with comparative measurements for Pb, Fe, Al, Cu determined with ETV-ICP-MS in another laboratory (Frech, W., Björn, E., Department of Analytical Chemistry, Umea, Sweden). For this purpose, part of the loaded platforms was analyzed in the authors' lab; others were sent by post to the external lab for comparative measurements. In addition to the SEM, information about element content of certain single particles can be obtained with micro-probing by detecting the wavelength- or energy-dispersed X-ray emission (EDX) excited with the electron beam. In general, the full information obtained with EP samples that are simultaneously collected on different substrates with the 10-fold-sampler, total element composition, particle size, structure, and composition, may be a testifying fingerprint for identifying the origin of the respective particulates.

SEMs with an atmospheric aerosol sampled on the institute roof windward in the outskirts urban area of Giessen are shown in Figs. 8a–c. In this case, sampling time was 45 min, the air volume 6.75 l, only. Determinations with multielement ETV-CFS yielded the contents: 6 ng Fe, 0.8 ng Al, and 0.4 ng Cu, corresponding to the concentrations: 890 ng/m³ Fe,

Table 1: Analytical results measured with ETV-Multi-element-CFS and with ETV-ICP-MS

Date	9. Oct. 2000	10. Oct. 2000	11. Oct. 2000	12. Oct. 2000
Sampling time	5 h	8 h	6 h	2 h
Air volume	45 L	72 L	54 L	18 L
Multi-element CS-CFS Number of samples	4	4	(1)	4
Fe (302,1), ng/m ³	61 ± 21	30 ± 11	(146)	109 ± 67
Mn (279,8), ng/m ³	2,6 ± 0,9	2,2 ± 1,4	not determined	not determined
Al (308,2), ng/m ³	35 ± 9	29 ± 11	(65)	88 ± 43
Cu (324,8), ng/m ³	11 ± 7	31 ± 13	(68)	172 ± 85
ETV-ICP-MS Number of samples	2	2	7	2
Pb, ng/m ³	11,3	6,7 ± 0,5	7,5 ± 0,3	15,8 ± 5,1
Fe, ng/m ³	91 ± 53	28,5 ± 1	54 ± 33	180 ± 27
Al, ng/m ³	12,9 ± 1,6	7 ± 0,7	9,6 ± 3,6	29 ± 9
Cu, ng/m ³	37 ± 26	22 ± 13	18 ± 9	(1027 ± 430)

Further contents: Si (CFS auf $\lambda = 288,2$ nm signals saturated), Ca (422,7): >70 ng/m³, Mg (285,2): >9 ng/m³

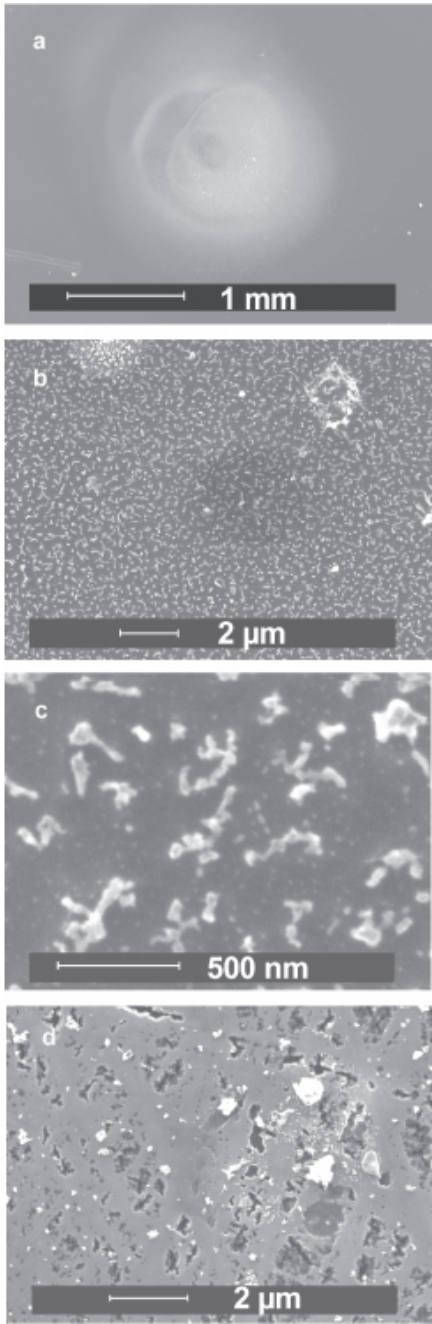


Fig. 8: Micrographs of) aerosol particles (Philips XL 30). a–c) precipitated in a outskirts urban area. d) indoors in a laboratory room

119 ng/m³ Al, and 59 ng/m³ Cu. Further samples were collected, one after the other, with a single-sample collector in the mechanical institute workshop during times of low working activity, i.e. at different times during the same day. One set of samples was analyzed with ETV-CS-CFS, another set was sent to Analytik Jena AG and analyzed for iron with an 'AAS 5 solid' SSAAS instrument that is specially dedicated for solid sampling with the boat technique. Results were in the range 320–1160 ng/m³ and 410–1750 ng/m³ Fe, respectively. **Fig. 8d** presents a SEM of a sample collected in a

laboratory that was not used since several weeks. On this micrograph particles with higher (bright) as well as with lower electron reflectivity (dark) are seen.

The investigations show that EP is well suitable to construct a low-volume precipitator as a single- or a multiple-sampler. Substrates of silicon, HOPC, or GC are right to collect particulates for microscopic analysis of the particle size and structure. Graphite boats as used as standard platforms in ETAAS instruments are proper sample collectors and sample introduction boats for all modern instrumental and approaches of element analyses. Aerosol contents of a few litres of air are sufficient to obtain masses in the analytical ranges of common instruments. Results with exchanging sampling boats by mailing them by post to other laboratories in simple polyethylene containers have proven the high stability of the surface bound samples.

The results show that direct solid sampling of aerosols in combination with methods of modern instrumental analyses is much more sensitive on masses and mass composition than classical gravimetric methods and leads to much more differentiated information. The presented measurements show a relatively high scatter and standard deviations. As reasons leakages of sealings and O-rings, shortcomings with the dosing valves, misalignment of the discharge tip, and moistness in the HV zone of the precipitators, rather than principle problems are taken into account. Therefore, the new improved sampler described in section 2 has been constructed. Owing to the promising results with electrostatic precipitation, a high-volume sampler based on EP in a metal tube that will be installed subsequently to the cyclone of Ref. [3] has been constructed and shall be tested. The results of the new developments will be published in a future paper.

6 Conclusions

For chemical and microscopic analysis, atmospheric aerosols can be electrostatically collected onto miniature substrates of 4–5 mm in width. Directing the aerosol flow against the electrically conductive surface of the collecting substrate and exciting a corona discharge of 10–15 μA above its surface can achieve the precipitation achieved quantitatively.

As collectors, boats and platforms as commonly used for solid sampling analytical instruments can be employed. Thereby, the sampling technique is suited for elemental analysis with all modern analytical instruments, which allow direct solid sampling without preceding digestion by using acids and reagents that are to be disposed later. The reusable graphite sampling boats easily can be cleaned by a simple heating step. For SEM and EDX, platforms cut from silicon wavers, HOPC, GC could be successfully employed, or glass plates with conductive layers of ITO for optical microscopy.

Owing to the miniature size of the precipitators, a ten-fold precipitator could be constructed which simultaneously collects the particulates on up to ten substrates of same or different types for analyzing with different microscopic or instrumental chemical analyses approaches or for doing dif-

ferent determinations by using sequential methods. Furthermore, the miniature size of the sample and of the boats will be optimal for automated instrumentation and for men carried constructions. Direct solid sampling of aerosol particulates in combination with methods of modern instrumental analyses results in more sensitivity than classical gravimetry and gives more differentiated information. The boats with surface adsorbed samples are stable for storage and transport.

The experience from the field and firmness testing was taken into account for constructing a new improved sampling apparatus. The results will be reported in a future paper.

Acknowledgements. The authors are indebted to the Deutsche Bundesstiftung Umwelt (DBU) for financial support, to Prof. Dr. H. M. Ortner, Dr. M. Heck, and Dipl. Ing. B. Höflich and Dipl. Ing. J. Saroukh of the Technische Universität Darmstadt, Darmstadt, Germany, for the micrographs with SEM Philips XL 30, furthermore, to Dr. M. Hardt, 'Zentrale Biotechnische Betriebseinheit' for those with SEM Philips XL 20 as well as to Prof. Dr. R. Gruehn and Dr. W. Mertin, Institut für Anorganische Chemie, University Giessen, for those with TEM, to Prof. Dr. W. Frech, Dr. E. Björn, Department of Chemistry, University of Umea, Sweden, for ETV-ICP-MS measurements, to Analytik Jena AG, Jena, Germany, for SSAAS measurements, and to Schunk Kohlenstoffwerke GmbH, Heuchelheim, Germany, for support with graphite parts.

References

- [1] Hinds CW (1999): *Aerosol Technology – Properties, behavior, and measurement of airborne particles*. 2nd Edition, John Wiley & sons, New York
- [2] Lüdke C, Hoffmann E, Skole J, Kriew M (1999): Determination of trace metals in size fractionated particles from arctic air by electrothermal vaporization inductively coupled plasma mass spectrometry. *J. Anal. At. Spectrom.* **14**, 1685–1690
- [3] Jaeschke W, Fuchs J, Ift F, Krause H (2002): Development and Test of a New Monitor for Atmospheric Carbonaceous Particles. *ESPR – Environ Sci & Polut Res* Vol. 9, Special Issue 4, pp 109–116 (this issue)
- [4] Torge R: private communication
- [5] Welz B, Sperling M (1998): *Atomic Absorption Spectrometry*. 3. Edition, Wiley-VCH, Weinheim
- [6] Torge R (1980): *Carl Zeiss Oberkochen: research report*
- [7] Kurfürst U, Rues B (1981): *Fresenius Z. Anal. Chem.* **308**, 1–6
- [8] Kurfürst U (1997): *Solid Sample Analysis – Direct and Slurry Sampling using ETAAS and ETV-ICP*, Springer, Heidelberg
- [9] Boonen S, Vanhaeke L, Moens L, Dams R (1996): Direct determination of Se and As, in solid certified reference materials using electrothermal vaporization inductively coupled plasma mass spectrometry. *Spectrochim. Acta B* **51**, 271–278
- [10] Kantor T (2000): Sample introduction with graphite furnace electrothermal vaporization into an inductively coupled plasma: effects of streaming conditions and gaseous phase additives. *Spectrochim. Acta B* **55**, 431–448
- [11] Hermann G (1992): Coherent Forward Scattering Atomic Spectrometry. *Anal. Chem.* **64**, 571A–579A
- [12] Bernhard J, Hermann G, Lasnitschka G (1999): Simultaneous multi-element determination with coherent forward scattering spectrometry employing chromatically corrected polarizers and a fast scacing spectrometer. *Spectrochim. Acta B* **54**, 645–656
- [13] Buchkamp T, Hermann G (1999): Solid sampling by electrothermal vaporization in combination with electrostatic particle deposition for electrothermal atomization multi-element analysis. *Spectrochim. Acta B* **54**, 657–668
- [14] Buchkamp T, Garbrecht A, Hermann G, Kling B (1997): Size and distribution of particles deposited electrostatically onto the platform of a graphite furnace using laser ablation sampling. *Spectrochim. Acta B* **52**, 1525–1533
- [15] Chen DR, Pui DYH, Hummes D, Fissan H, Quant FR, Sem GJ: (1998): Design and Evaluation of a Nonometer Aerosol Differential Mobility Analyzer (Nano-DMA). *J. Aerosol Sci.* **29**, 497–509
- [16] Kämpfer P (2001): Institute for Applied Microbiology, Justus-Liebig-University Giessen, private communication